Modes in Dielectric-Loaded Waveguides and Resonators

KAWTHAR A. ZAKI AND ALI E. ATIA, SENIOR MEMBER, IEEE

Abstract—**Analysis of nonaxially symmetric modes in circular waveguides partially filled with high-dielectric constant material is presented. A method for the accurate determination of resonant frequencies of any mode excited in dielectrically loaded waveguide cavities is described. The method is used to construct mode charts for dielectric resonators. Comparison of the resonant frequency calculations for several cases agrees closely with measurements.**

I. Introduction

THE RECENT AVAILABILITY of low-loss, temperature-stable high-dielectric constant materials [1] has generated increased interest in the utilization of such materials in several microwave components. Major factors in the use of high-dielectric constant materials are the miniaturization of the components, lower manufacturing and production costs, and the potential compatibility with microwave integrated circuits (MIC's) and monlolithic microwave integrated circuits (MMIC's). One of the most interesting applications of dielectric resonators is in high-quality dual mode bandpass filters [2]. The design of such filters requires the accurate computation of the resonant frequency of practical resonator configurations. Although several authors [3]–[6] have presented methods for the computation of the resonant frequencies of dielectric resonators excited in axially symmetric modes (i.e., $TE_{01\delta}$ or $TM_{01\delta}$ modes), taking into account mounting structures and enclosures, there is virtually no treatment of other nonaxially symmetric modes in the literature. Properties of these modes are required for successful design of resonators, both when these modes are in the design, or when they are potentially excited as spurious modes.

This paper describes a rigorous method for the computation of the resonant frequencies and fields of dielectric resonators excited in nonaxially symmetric modes. The analysis of axially symmetric and hybrid modes in partially filled infinite waveguides is reviewed in Section II, since the properties of these modes are required for the subsequent treatment of the resonant modes. The method of computing the resonant frequencies of dielectric resonators enclosed in circular waveguides is described in Section III. This method is applied to construct mode charts for resonators of typical parameters. Results on the computation of the resonant frequencies of several resonators are presented in Section IV, together with a mode chart for a representative case.

Manuscript received April 6, 1983; revised August 4, 1983.

K. A. Zaki is with the Electrical Engineering Department, University of Maryland, College Park, MD 20742.

A. L. Atia is with the Communications Satellite Corporation, 950 L'Enfant Plaza, S.W. Washington, D.C. 20024

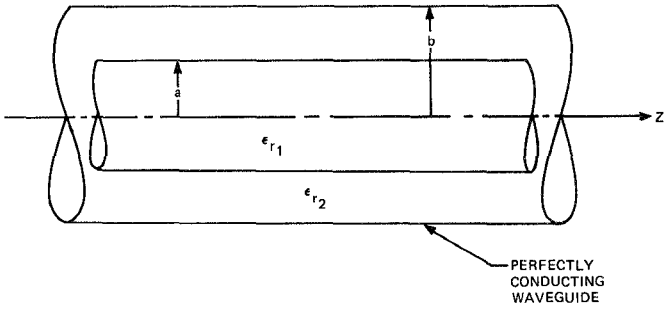

Fig. 1. Dielectrically loaded waveguide.

II. Modes in Dielectric-Loaded Circular Waveguides

This section summarizes the results of solving Maxwell's equations in a circular waveguide partially filled with a dielectric material. The circular waveguide of infinite extent has radius b, and is axially loaded with a concentric dielectric of circular cross section, radius a, and relative dielectric constant ϵ_{r_1}, as shown in Fig. 1. The space between the perfectly conducting wall of the waveguide and the dielectric core is filled with another dielectric of relative permittivity $\epsilon_{r_2} \ll \epsilon_{r_1}$. The electromagnetic fields which can exist within this structure are (see, for example, [7]–[9]): 1) transverse electric modes with no angular variation of the fields (TE_{0m} modes), 2) transverse magnetic modes with no angular variation of the fields (TM_{0m} modes), and 3) hybrid modes which have both axial electric and magnetic fields and angular variation of the fields (HE_{nm} modes, $m, n \neq 0$).

Suppressing the axial propagation factor $e^{-\gamma z}$ and time variation factor $e^{j\omega t}$, the solution to the boundary value problem leads to the field components of the HE_{nm} modes given below.

For $0 \leqslant r \leqslant a$

$$E_{z_1} = AJ_n(\xi_1 r)\cos n\phi \tag{1a}$$

$$j\omega\mu H_{z_1} = \alpha A J_n(\xi_1 r)\sin n\phi \tag{1b}$$

$$E_{r_1} = \frac{-A}{\xi_1^2}\left[\gamma\xi_1 J_n'(\xi_1 r) + \frac{\alpha n J_n(\xi_1 r)}{r}\right]\cos n\phi \tag{1c}$$

0018-9480/83/1200-1039$01.00 ©1983 IEEE

and

$$E_{\phi_1} = \frac{A}{\xi_1^2}\left[\frac{\gamma n J_n(\xi_1 r)}{r} + \alpha \xi_1 J_n'(\xi_1 r)\right]\sin n\phi \tag{1d}$$

$$j\omega\mu H_{r_1} = \frac{A}{\xi_1^2}\left[\frac{nk_1^2 J_n(\xi_1 r)}{r} - \alpha\gamma\xi_1 J_n'(\xi_1 r)\right]\sin n\phi \tag{1e}$$

$$j\omega\mu H_{\phi_1} = \frac{-A}{\xi_1^2}\left[-k_1^2\xi_1 J_n'(\xi_1 r) + \frac{\alpha\gamma n J_n(\xi_1 r)}{r}\right]\cos n\phi. \tag{1f}$$

For $a \leqslant r \leqslant b$

$$E_{z_2} = AR_n(\zeta_2 r)\cos n\phi \tag{2a}$$

$$j\omega\mu H_{z_2} = \alpha A P_n(\zeta_2 r)\sin n\phi \tag{2b}$$

$$E_{r_2} = \frac{A}{\zeta_2^2}\left[\zeta_2\gamma R_n'(\zeta_2 r) + \alpha n\frac{P_n(\zeta_2 r)}{r}\right]\cos n\phi \tag{2c}$$

$$E_{\phi_2} = \frac{-A}{\zeta_2^2}\left[\frac{\gamma n R_n(\zeta_2 r)}{r} + \alpha\zeta_2 P_n'(\zeta_2 r)\right]\sin n\phi \tag{2d}$$

$$j\omega\mu H_{r_2} = \frac{-A}{\zeta_2^2}\left[\frac{nk_2^2 R_n(\zeta_2 r)}{r} - \alpha\gamma\zeta_2 P_n'(\zeta_r r)\right]\sin n\phi \tag{2e}$$

$$j\omega\mu H_{\phi_2} = \frac{A}{\zeta_2^2}\left[-k_2^2\zeta_2 R_n'(\zeta_2 r) + \frac{\alpha\gamma n P_n(\zeta_2 r)}{r}\right]\cos n\phi \tag{2f}$$

where A is an arbitrary constant, and

$$\xi_1^2 = k_1^2 + \gamma^2, \quad \zeta_2^2 = -\left(k_2^2 + \gamma^2\right)$$

$$k_1^2 = \epsilon_{r_1}k_0^2, \quad k_2^2 = \epsilon_{r_2}k_0^2, \quad k_0^2 = \omega^2\mu_0\epsilon_0$$

$$P_n(\zeta_2 r) = J_n(\xi_1 a)\left[\frac{K_n(\zeta_2 r)I_n'(\zeta_2 b) - I_n(\zeta_2 r)K_n'(\zeta_2 b)}{K_n(\zeta_2 a)I_n'(\zeta_2 b) - I_n(\zeta_2 a)K_n'(\zeta_2 b)}\right]$$

$$R_n(\zeta_2 r) = J_n(\xi_1 a)\left[\frac{K_n(\zeta_2 r)I_n(\zeta_2 b) - I_n(\zeta_2 r)K_n(\zeta_2 b)}{K_n(\zeta_2 a)I_n(\zeta_2 b) - I_n(\zeta_2 a)K_n(\zeta_2 b)}\right]$$

$$\alpha = \frac{-U_n}{aV_n}$$

$$U_n = n\gamma a J_n(\xi_1 a)\left[\frac{1}{\xi_1^2 a^2} + \frac{1}{\zeta_2^2 a^2}\right]$$

$$V_n = \left[\frac{J_n'(\xi_1 a)}{\xi_1 a} + \frac{P_n'(\zeta_2 a)}{\zeta_2 a}\right]$$

and $J_n(\cdot)$, $I_n(\cdot)$, and $K_n(\cdot)$ are the Bessel functions, and modified Bessel functions of the first and second kinds, respectively.

The characteristic equation for the normalized radial wavenumber $x_{nm} = \xi_1 a$ (from which the propagation constant γ can be computed) is

$$U_n^2 + k_0^2 a^2 V_n W_n = 0 \tag{3}$$

where

$$W_n = \left[\epsilon_{r_1}\frac{J_n'(\xi_1 a)}{\xi_1 a} + \epsilon_{r_2}\frac{R_n'(\zeta_2 a)}{\zeta_2 a}\right].$$

The characteristic equations for the propagation constants of the axially symmetric modes (TE_{0m} and TM_{0m}) are given, respectively, by

$$W_0 = 0 \ (TE_{0m} \text{ modes})$$

$$V_0 = 0 \ (TM_{0m} \text{ modes}).$$

The nonvanishing components of these axially symmetric modes are given below.

TE_{0m} modes:

For $0 \leqslant r \leqslant a$

$$H_{z_1} = AJ_0(\xi_1 r) \tag{4a}$$

$$E_{\phi_1} = \frac{j\omega\mu}{\xi_1}AJ_0'(\xi_1 r) \tag{4b}$$

$$H_{r_1} = \frac{-\gamma}{\xi_1}AJ_0'(\xi_1 r). \tag{4c}$$

For $a \leqslant r \leqslant b$

$$H_{z_2} = -A\frac{\zeta_2 J_0'(\xi_1 a)}{\xi_1 J_0(\xi_1 a)}P_0(\zeta_2 r) \tag{5a}$$

$$E_{\phi_2} = j\omega\mu A\frac{J_0'(\xi_1 a)}{\xi_1 J_0(\xi_1 a)}P_0'(\zeta_2 r) \tag{5b}$$

$$H_{r_2} = \frac{-\gamma}{\xi_1}\frac{J_0'(\xi_1 a)}{J_0(\xi_1 a)}P_0'(\zeta_2 r). \tag{5c}$$

TM_{0m} modes:

For $0 \leqslant r \leqslant a$

$$E_{z_1} = AJ_0(\xi_1 r) \tag{6a}$$

$$E_{r_1} = \frac{-A\gamma}{\xi_1}J_0'(\xi_1 r) \tag{6b}$$

$$H_{\phi_1} = \frac{j\omega\epsilon_1}{\xi_1}AJ_0'(\xi_1 r). \tag{6c}$$

For $a \leqslant r \leqslant b$

$$E_{z_2} = AR_0(\zeta_2 r) \tag{7a}$$

$$E_{r_2} = A\frac{\gamma}{\zeta_2}R_0'(\zeta_2 r) \tag{7b}$$

$$H_{\phi_2} = \frac{j\omega\epsilon_2}{\zeta_2}R_0'(\zeta_2 r). \tag{7c}$$

III. Dielectric-Loaded Waveguide Resonators

Waveguide cavities are usually used in applications requiring high-Q microwave resonators. Waveguide components are generally bulky, heavy, and expensive to manufacture due to the high precision required in their machining operations. A means for the potential size reduction of the resonators is to fill them with a high-dielectric constant, low-loss material. The reduction in the linear dimensions of the components would be proportional to $\sqrt{\epsilon_r}$. The metallic enclosure losses, however, would increase considerably, since the surface area in which the currents flow are reduced by ϵ_r. Alternatively, the enclosure conducting walls can be made remote from the resonator

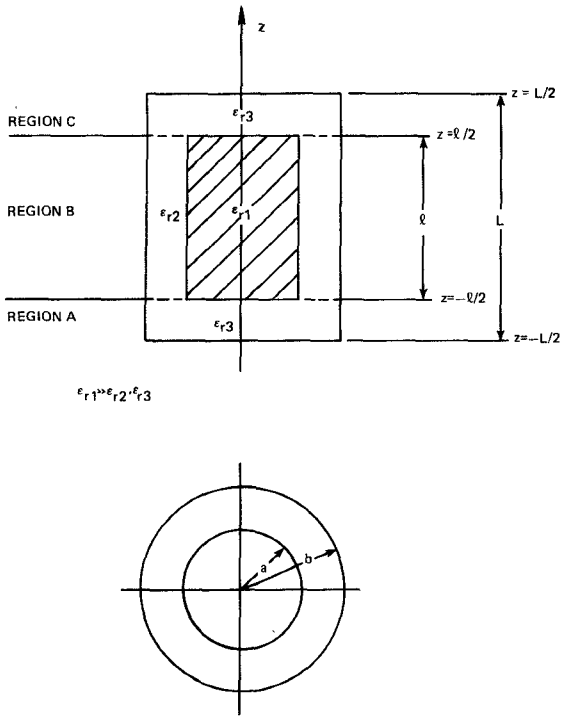

Fig. 2. Dielectric-loaded circular cavity.

which would contain most of the fields. This allows the ohmic losses in the enclosure walls to be significantly reduced. The resonator fields and resonant frequencies in this case are generally significantly different from what would exist in a full resonator.

In this section, a method is presented for the accurate determination of the resonant frequency of the structure shown in Fig. 2. The cavity of radius b and length L has perfectly conducting walls. The high relative dielectric constant cylinder (ϵ_{r_1}) has radius a and length l, and is supported by low relative dielectric constant support (ϵ_{r_2}) (e.g., foam). This support can conveniently be made as two half-cups, between which the resonator is sandwiched. Alternatively, the end supports can be of different dielectric constant material (ϵ_{r_3}), as shown in Fig. 2.

To compute the resonant frequency, the structure is divided into three regions: A, B, and C, as indicated in Fig. 2. In each of these regions, the total fields are expressed in terms of a linear combination of the appropriate normal waveguide modes. The transverse electric and magnetic fields are then matched at the boundaries $z = \pm l/2$. This results in an infinite set of linear homogeneous equations. Resonant frequencies of the structure are determined by equating to zero the determinant of a truncated subset of these equations.

The normal modes in the end regions (A and C) are the usual TE and TM modes in a circular waveguide [10]. Region B fields are those described in the previous section. The angular variation of the fields of a particular resonant mode must be the same in all three regions. The transverse fields in each of the three regions A, B, and C, which satisfy the boundary conditions of vanishing electric field tangential to the end face $z = \pm L/2$, are expressed as

$$\boldsymbol{E}_A = \sum_i a_i \hat{e}_i \sinh\gamma_i (L/2 + z) \tag{8a}$$

$$\boldsymbol{H}_A = -\sum_i a_i \hat{h}_i \cosh\gamma_i (L/2 + z) \tag{8b}$$

$$\boldsymbol{E}_B = \sum_i \hat{E}_i (A_i e^{-\gamma_i z} + B_i e^{\gamma_i z}) \tag{9a}$$

$$\boldsymbol{H}_B = \sum_i \hat{H}_i (A_i e^{-\gamma_i z} - B_i e^{\gamma_i z}) \tag{9b}$$

$$\boldsymbol{E}_C = \sum_i b_i \hat{e}_i \sinh\gamma_i (L/2 - z) \tag{10a}$$

$$\boldsymbol{H}_C = \sum_i b_i \hat{h}_i \cosh\gamma_i (L/2 - z) \tag{10b}$$

where γ_i, $\hat{e}_i$, and $\hat{h}_i$ are the propagation constants, transverse electric, and magnetic fields of the normal modes (i.e., TE or TM modes) in the circular waveguide of radius b, respectively, and γ_i, $\hat{E}_i$, and $\hat{H}_i$ are the propagation constants, transverse electric, and magnetic fields of the (hybrid) modes in the dielectric loaded waveguide, respectively. The γ_i's are roots of (3), while $\hat{E}_i$ and $\hat{H}_i$ are the fields given by (1) and (2).

Boundary conditions to be satisfied by the fields of (8)–(10) are that the transverse electric and magnetic fields be continuous at $z = \pm l/2$, i.e., at $z = -l/2$

$$\boldsymbol{E}_A = \boldsymbol{E}_B, \quad \boldsymbol{H}_A = \boldsymbol{H}_B \tag{11a}$$

and at $z = l/2$

$$\boldsymbol{E}_B = \boldsymbol{E}_C, \quad \boldsymbol{H}_B = \boldsymbol{H}_C. \tag{11b}$$

Taking the dot product of each of the electric field equations (11a) and (11b), with $\hat{e}_j$, and the magnetic field equations with $\hat{h}_j$ and integrating over the waveguide cross section, using the orthogonality relations of the normal modes [10], the following set of homogeneous linear equations result:

$$a_j s_j = \sum_i (A_i e^{\gamma_i l/2} + B_i e^{-\gamma_i l/2}) \langle \hat{E}_i, \hat{e}_j \rangle \tag{12a}$$

$$-a_j c_j = \sum_i (A_i e^{\gamma_i l/2} - B_i e^{-\gamma_i l/2}) \langle \hat{H}_i, \hat{h}_j \rangle \tag{12b}$$

$$b_j s_j = \sum_i (A_i e^{-\gamma_i l/2} + B_i e^{\gamma_i l/2}) \langle \hat{E}_i, \hat{e}_j \rangle \tag{12c}$$

$$b_j c_j = \sum_i (A_i e^{-\gamma_i l/2} - B_i e^{\gamma_i l/2}) \langle \hat{H}_i, \hat{h}_j \rangle \tag{12d}$$

where

$$\langle \hat{E}_i, \hat{e}_j \rangle = \int_S \hat{E}_i \cdot \hat{e}_j^* \, dS \tag{13a}$$

$$\langle \hat{H}_i, \hat{h}_j \rangle = \int_S \hat{H}_i \cdot \hat{h}_j^* \, dS \tag{13b}$$

$$s_j = \sinh\gamma_j \left(\frac{L-l}{2}\right), \quad c_j = \cosh\gamma_j \left(\frac{L-l}{2}\right).$$

Analytic expressions for the inner product terms of (13a) and (13b) are given in the Appendix.

The a_j's and b_j's can be easily eliminated from

(12a)–(12d), leaving the system of equations only in A_t's and B_t's

$$\sum_t \left(X_{jt} A_t + Y_{jt} B_t \right) = 0 \tag{14a}$$

$$\sum_t \left(Y_{jt} A_t + X_{jt} B_t \right) = 0 \tag{14b}$$

where

$$X_{jt} = e^{\gamma_t l/2} \left[c_j \langle \hat{E}_t, \hat{e}_j \rangle + s_j \langle \hat{H}_t, \hat{h}_j \rangle \right] \tag{15a}$$

$$Y_{jt} = e^{-\gamma_t l/2} \left[c_j \langle \hat{E}_t, \hat{e}_j \rangle - s_j \langle \hat{H}_t, \hat{h}_j \rangle \right]. \tag{15b}$$

The resonant frequencies of the structure are the roots of the equation

$$\det \begin{bmatrix} X & Y \\ Y & X \end{bmatrix} = 0 \tag{16}$$

where the element values of the submatrices X and Y (X_{jt} and Y_{jt}) are given by (15a) and (15b). In practice, the infinite matrices X and Y are truncated at a certain number N of normal waveguide and hybrid modes. Then the frequency is varied and the value of the determinant in (16) is computed for each frequency. The frequencies giving zero value of the determinant are approximations to the resonant frequencies. The size of the determinant N can be varied, and the process can be repeated to establish the convergence.

A flow chart of a computer program that implements this procedure is shown in Fig. 3. This program uses the bisection method to compute the resonant frequencies, once the upper and lower bounds on the values of the frequencies are known. Such bounds are easily estimated using the dielectric-loaded waveguide model shorted at both ends with lengths l and L for the upper and lower bounds, respectively.

The frequencies obtained by this method are the resonances of the structure in various modes. Thus, "mode charts" can be constructed which show the variation of various resonant frequencies with the parameters of the resonator (e.g., diameter and length of the dielectric, diameter and length of the cavity, etc.). When only one hybrid and one normal waveguide mode are taken (i.e., $N=1$), (16) reduces to

$$\tanh \gamma l = \frac{-\sinh \gamma (L-l)}{\dfrac{\langle \hat{E}, \hat{e} \rangle}{\langle \hat{H}, \hat{h} \rangle} \cosh^2 \gamma \dfrac{(L-l)}{2} + \dfrac{\langle \hat{H}, \hat{h} \rangle}{\langle \hat{E}, \hat{e} \rangle} \sinh^2 \gamma \dfrac{(L-l)}{2}}. \tag{17}$$

This equation gives the exact values of the resonant frequencies when $L = l$.

An interesting interpretation of (17) can be made in a simple way by considering the "equivalent circuit" shown in Fig. 4. In this figure, the transmission line of length l, characteristic impedance Z_0, and propagation constant γ represent the hybrid mode in the loaded waveguide, while the lines of lengths $(L-l)/2$, characteristic impedances $\bar{Z}_0$, and propagation constants $\bar{\gamma}$ represent the normal

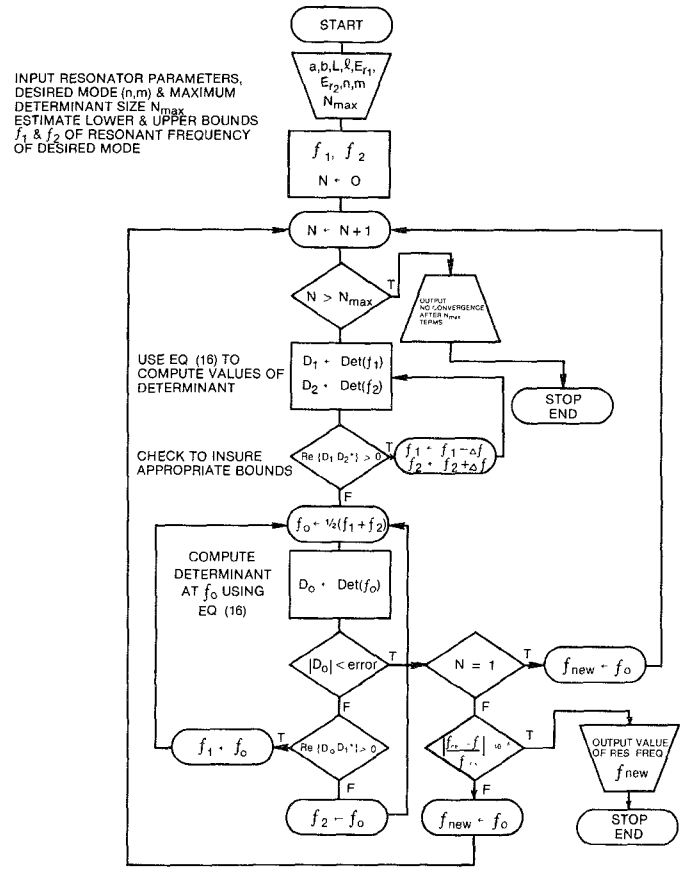

Fig. 3. Flow chart of a computer program for resonant frequency calculations.

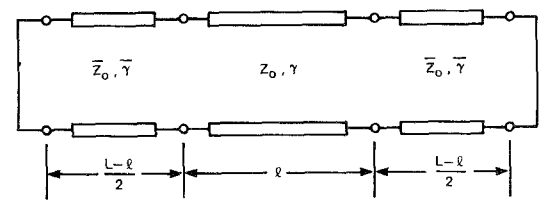

Fig. 4. Equivalent circuit of a dielectric-loaded resonator.

waveguide mode, terminated in short circuits at their ends. Using the transmission-line equations, it can be easily shown that the resonant frequencies of the circuit of Fig. 4 are given by (17), provided that

$$\frac{Z_0}{\bar{Z}_0} = \frac{\langle \hat{E}, \hat{e} \rangle}{\langle \hat{H}, \hat{h} \rangle}. \tag{18}$$

IV. Results

Accuracy of the computer program developed for the solution of the characteristic equation was verified by using the program to find the roots of the equation with $\epsilon_{r_1} = \epsilon_{r_2}$, which corresponds to a completely full waveguide. These roots ($\xi_1 b$) agreed with the TE and TM normal mode wavenumbers (i.e., roots of $J_n'(x) = 0$ or $J_n(x) = 0$) to six decimal places.

Properties of the modes in an infinite waveguide axially loaded with a dielectric are first explored by investigating the characteristic equation (3). Since the highly tempera-

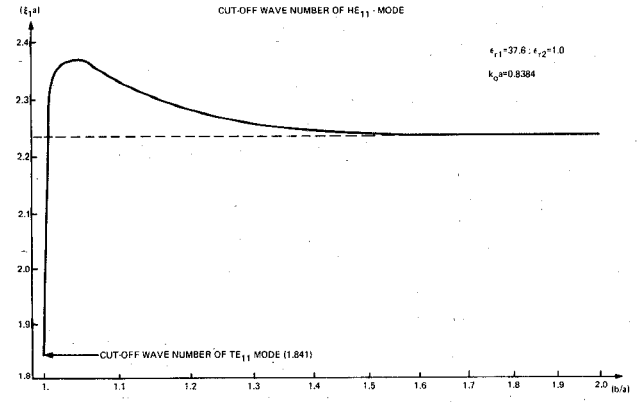

Fig. 5. Effect of the waveguide radius on the HE_{11} mode cutoff wavenumbers.

TABLE I
ROOTS OF THE CHARACTERISTIC EQUATION FOR TE_{0m}, TM_{0m}, AND HE_{nm} MODES

Mode	Root	Mode	Root
HE_{11}	2.2607	HE_{23}	6.6963
TM_{01}	3.4542	HE_{31}	6.7949
HE_{21}	3.6865	TE_{02}	7.0296
TE_{01}	3.7863	HE_{14}	7.1294
HE_{12}	4.4053	HE_{32}	8.0237
HE_{13}	5.3516	HE_{24}	8.2617
HE_{22}	5.8555	TM_{03}	8.4158
TM_{02}	5.8988	HE_{15}	8.5313
		HE_{33}	9.3281

a = 0.394", b = 0.5", k_0a = 0.8384"

ture-stable dielectric materials commercially available have relative dielectric constants in the range 35–40, a typical value of $\epsilon_{r_1} = 37.6$ is used in the calculations. The first few roots $(\xi_1 a)$ of the characteristic equation (3) for a typical set of parameters are given in Table I. Variation of the cutoff wavenumber $(\xi_1 a)$ of the hybrid HE_{11} mode with the ratio (b/a) is shown in Fig. 5. As seen in this figure, when $b/a = 1$, the waveguide is completely full of dielectric and the mode is TE_{11} with cutoff wavenumber 1.841. As the waveguide diameter is increased, the cutoff wavenumber of the HE_{11} mode increases rapidly and peaks around $(b/a) = 1.07$. In the range $(b/a) < 1.3$, the effect of the conducting walls on the fields is significant due to their proximity to the dielectric. For $(b/a) > 1.5$, the cutoff wavenumber of the HE_{11} mode is virtually independent of (b/a), indicating the fields are almost entirely concentrated within the dielectric core, and only weak evanescent fields exist near the conducting walls. This is also illustrated in the $\omega - \beta$ diagram of Fig. 6 for the hyrid HE_{11} mode. Thus, in the design of the HE_{11} mode resonator with relative dielectric constants in the range of 35–40, the waveguide radius b should be generally chosen greater than $1.5 \times$ the dielectric radius a to minimize the waveguide conductor loss.

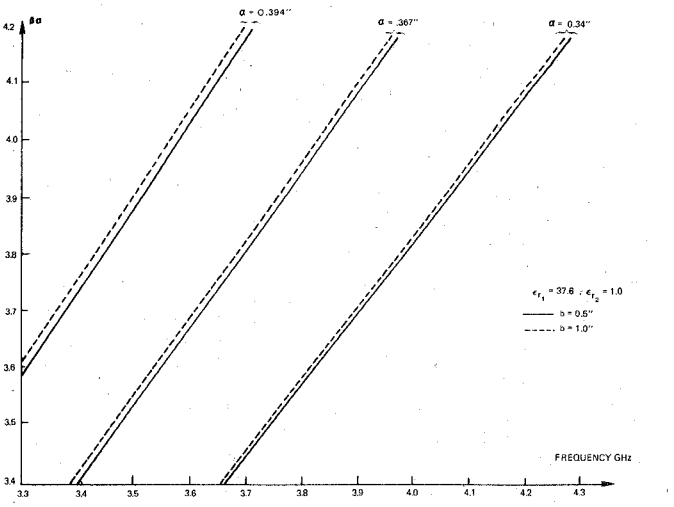

Fig. 6. Omega–beta diagrams for the HE_{11} mode.

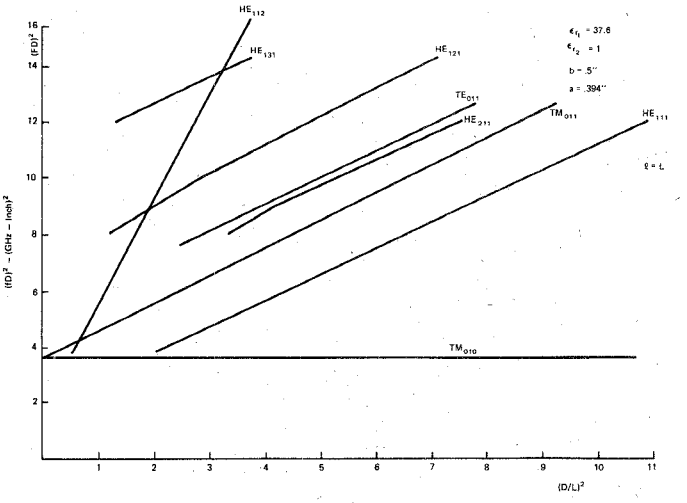

Fig. 7. Mode chart for a dielectric-loaded waveguide resonator.

TABLE II
COMPUTED AND MEASURED RESONANT FREQUENCIES OF SEVERAL RESONATORS

a"	b"	ℓ"	L"	ϵ_{r_1}	Frequency (Measured) MHz	Frequency (Computed) MHz
.394	.5	.315	.6	37.6	3368	3371
.341	.5	.319	.83	37.25	3928	3930
.315	.5	.272	.56	37.6	4196	4192
.268	.5	.220	.48	38.2	4994	5001

A mode chart for a dielectric-loaded cavity of the same parameters given in Table I, with $l = L$, is shown in Fig. 7. The plots of $(fD)^2$ versus $(D/L)^2$, where $D = 2a$ is the dielectric diameter, are almost straight lines, similar to the case of the homogeneously filled waveguide [11]. It is recognized that the chart of Fig. 7 is for the case where the dielectric extends all the way to the end plates (and hence the modes existing in the resonators are only "pure

modes"), yet it does give a quantitative measure of the other modes, which would exist when $L > l$.

Finally, a comparison of measured results of the resonant frequencies of several resonators (given in [2]) with the computed values using (17) is given in Table II. The agreement between the measured and computed values using the technique presented above is quite good.

V. Conclusions and Discussions

The rigorous method presented for the computation of the resonant frequencies of dielectric-loaded waveguide resonators is shown to be capable of providing quite accurate results. The method uses the mode fields of an infinite dielectric-loaded waveguide with the same cross section as the cavity; hence, the fields are quite similar to those actually existing in the cavity, except within the regions near the ends, in which the normal TE and TM empty waveguide modes are used. The cutoff wavenumbers presented in Table I should be useful in the initial determination of practical resonator dimensions in the types of dielectric materials presently available. The method is applicable for both axially symmetric and nonsymmetric modes. An example of a mode chart for a dielectric-loaded waveguide resonator is given showing the variation of the resonant frequency of various modes with the resonator dimensions. This mode chart is found to be similar in shape to the case of homogeneously filled waveguide cavities.

Appendix
Analytic Expressions for the Inner Products of (13a) and (13b)

In the following expressions, k_c represents the cutoff wavenumbers of either a TE or TM mode in a circular waveguide of radius b and full of a dielectric material of relative permittivity ϵ_{r_2}. All the other quantities are as defined in the text.

Let

$$A = nJ_n(\xi_1 a)J_n(k_c a)\left(\frac{1}{\xi_1^2}+\frac{1}{\zeta_2^2}\right)$$

$$B = a\left[\frac{J_n(k_c a)J_n'(\xi_1 a)}{\xi_1} + \frac{\xi_1 J_n(k_c a)J_{n-1}(\xi_1 a) - k_c J_{n-1}(k_c a)J_n(\xi_1 a)}{k_c^2-\xi_1^2}\right]$$

$$C = \frac{a}{\zeta_2}\left[J_n(k_c a)P_n'(\zeta_2 a)\left(1+\frac{\zeta_2^2}{k_c^2+\zeta_2^2}\right) - \frac{\zeta_2 k_c}{k_c^2+\zeta_2^2}J_n(\xi_1 a)J_n'(k_c a)\right]$$

$$D = \frac{a}{\zeta_2}\left[J_n(k_c a)R_n'(\zeta_2 a)\left(1+\frac{\zeta_2^2}{k_c^2+\zeta_2^2}\right) - \frac{\zeta_2 k_c}{k_c^2+\zeta_2^2}J_n(\xi_1 a)J_n'(k_c a)\right].$$

Then

$$\langle \hat{E}, \hat{e}_{TE}\rangle = \frac{-1}{J_n(k_c a)}\sqrt{\frac{2\pi}{k_c^2 a^2 - n^2}}\,[\gamma A + \alpha(B+C)]$$

$$\langle \hat{H}, \hat{h}_{TE}\rangle = \frac{-j}{\omega\mu J_n(k_c a)}\sqrt{\frac{2\pi}{k_c^2 a^2 - n^2}} \cdot\left[\left(\frac{k_1^2\zeta_2^2 + k_2^2\xi_1^2}{\xi_1^2+\zeta_2^2}\right)A - \alpha\gamma(B+C)\right]$$

$$\langle \hat{E}, \hat{e}_{TM}\rangle = \frac{-\sqrt{2\pi}}{k_c a J_n'(k_c a)}\,[\alpha A + \gamma(B+D)]$$

$$\langle \hat{H}, \hat{h}_{TM}\rangle = \frac{j\sqrt{2\pi}}{\omega\mu k_c a J_n'(k_c a)}\left[-\alpha\gamma A + k_1^2 B - k_2^2 D\right].$$

References

[1] J. K. Plourde *et al.*, "Ba2 Ti_9 O_2 as a microwave dielectric resonator," *J. Amer. Ceram. Soc.*, vol. 58, no. 9–10, pp. 418–420, 1975.

[2] S. J. Fiedziuszko, "Dual-mode dielectric resonator loaded cavity filters," *IEEE Trans. Microwave Theory Tech.*, vol. MTT-30, pp. 1311–1316, Sept. 1982.

[3] S. Fiedziuszko and A. Jelenski, "The influence of conducting walls on resonant frequencies of the dielectric microwave resonator," *IEEE Trans. Microwave Theory Tech.*, vol. MTT-19, p. 778, Sept. 1971.

[4] R. R. Bonetti and A. E. Atia, "Design of cylindrical dielectric resonators in inhomogeneous media," *IEEE Trans. Microwave Theory Tech.*, vol. MTT-29, pp. 323–326, Apr. 1981.

[5] T. Itoh and R. Rudokas, "New method for computing the resonant frequencies of dielectric resonators," *IEEE Trans. Microwave Theory Techniques*, vol. MTT-25, pp. 52–54, Jan. 1977.

[6] P. Guillon, J. P. Balabaud, and Y. Garault, "TM_{01p} tubular and cylindrical dielectric resonator mode," in *Proc. 1981 IEEE MTT-S Internat. Microwave Symp.*, June 1981, pp. 163–166.

[7] L. Pincherle, "Electromagnetic waves in metal tubes filled longitudinally with two dielectrics," *Phys. Rev.*, vol. 66, pp. 118–130, Sept. 1944.

[8] L. G. Chambers, "Propagation in waveguides filled longitudinally with two or more dielectrics," *Brit. J. Appl. Phys.*, vol. 4, pp. 39–45, Feb. 1953.

[9] P. J. B. Clarricoats and B. C. Taylor, "Evanescent and propagating modes of dielectric-loaded circular waveguides," *Proc. Inst. Elec. Eng.*, vol. III, pp. 1951–1956, Dec. 1964.

[10] R. E. Collin, *Field Theory of Guided Waves*. New York: McGraw-Hill, 1960, ch. 5.

[11] G. G. Montgomery, *Techniques of Microwave Measurements*. New York: McGraw-Hill, 1947, sec. 5.4 and 5.5.

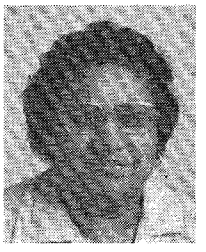

Kawthar A. Zaki received the B.S. degree with honors from Ain Shams University, Cairo, Egypt, in 1962, and the M.S. and Ph.D. degrees from the University of California, Berkeley, in 1966 and 1969, respectively, all in electrical engineering.

From 1962 to 1964, she was a Lecturer in the Department of Electrical Engineering, Ain Shams University. From 1965 to 1969, she held the position of Research Assistant in the Electronic Research Laboratory, University of California, Berkeley. She joined the Electrical Engineering Department, University of Maryland, College Park, MD, in 1970, where

she is presently an Associate Professor. Her research interests are in the areas of microwave circuits, optimization, and computer-aided design.

Dr. Zaki is a member of Tau Beta Pi.

Ali E. Atia (M'69–SM'78) received the B.Sc. degree from Ain Shams University, Cairo, Egypt in 1962, the M.S. and Ph.D. degrees from the University of California at Berkeley in 1966 and 1969, respectively, all in electrical engineering. From 1962 to 1964, he was a Lecturer in the Department of Electrical Engineering, Ain Shams University. From 1965 to 1969, he held the positions of Research Assistant and Assistant Professor in the Department of Electrical Engineering and Computer Science, University of California, Berkeley. He joined COMSAT Laboratories in 1969 where he was engaged in research and development activities on antennas and various microwave components and subsystems for satellite transponders. Currently, he is Senior Director for Satellite System Design for INTELSAT Technical Services, COMSAT's World System Division, where he directs system design and evaluation activities of current and future satellite systems for use by INTELSAT. Dr.

Dr. Atia is a member of Sigma Xi and of AIAA.

New Narrow-Band Dual-Mode Bandstop Waveguide Filters

JING-REN QIAN AND WEI-CHEN ZHUANG

Abstract —**A complementary relation between a dual-mode bandpass and bandstop waveguide filter is found. Then a new idea for constructing a bandstop filter is developed. Two trial samples of bandstop filters are constructed to demonstrate the principle.**

NOMENCLATURE

M_{ij}	Normalized coupling coefficient between the ith and the jth loop.
e_1	Equivalent source in the first loop.
Z	Impedance of each loop.
R, R_n	Equivalent loads in the first and last loop, respectively.
n	Number of the loops in Fig. 1.
i_k	Loop current in the kth loop.
$\boldsymbol{E}$	Voltage matrix for a bandpass filter circuit.
$\boldsymbol{Z}$	Impedance matrix for a bandpass filter circuit.
$\boldsymbol{I}$	Current matrix for a bandpass filter circuit.
R_0	Resistance looking into the source, characteristic impedance.
ω	Angular frequency.
e_0	Source voltage.
$\boldsymbol{S}$	A diagonal matrix.
$\boldsymbol{M}$	Coupling matrix.
$M'_{01}, M'_{n\,n+1}$	Normalized coupling coefficient between the main waveguide and the first loop and last loop, respectively.
m	Turn ratio of the ideal transformer.
i'_k	Loop current in the kth loop for a bandstop filter circuit.
e'_1, e'_n	Equivalent source in the first and last loop for a bandstop filter circuit, respectively.
R', R'_n	Equivalent load in the first and last loop for a bandstop filter circuit, respectively.
$\boldsymbol{E}'$	Voltage matrix for a bandstop filter circuit.
$\boldsymbol{Z}'$	Impedance matrix for a bandstop filter circuit.
$\boldsymbol{I}'$	Current matrix for a bandstop filter circuit.
$\boldsymbol{S}'$	A diagonal matrix.
t, r	Transmission and reflection coefficients for a bandpass filter.
t', r'	Transmission and reflection coefficients for a bandstop filter.
Δ, Δ'	Determinant of $\boldsymbol{Z}$ and $\boldsymbol{Z}'$, respectively.
$\Delta_{11}, \Delta_{1n}, \Delta_{nn}$	Co-factors of $\boldsymbol{Z}$.
$\Delta'_{11}, \Delta'_{1n}, \Delta'_{nn}$	Co-factors of $\boldsymbol{Z}'$.
V_{n-2}	Determinant of the $\boldsymbol{Z}$ matrix with first, last rows and first, last columns omitted.
V_n, V_{n-1}	Δ, Δ_{11} with $R = 0$, respectively.
θ, θ'	Arguments of t and t', respectively.
ω'_p, ω'_t	Relative frequency at the transmission pole and zero for a bandstop filter.

Manuscript received March 25, 1983; revised August 15, 1983.

J. -R. Qian is with the Department of Electrical Engineering, China University of Science and Technology, Hefei, Anhui, China.

W. -C. Zhuang is with Xian Institute of Radio Technology, Xian, Shanxi, China.

0018-9480/83/1200-1045$01.00 ©1983 IEEE